SHORT-PULSE DRIVEN PHOTOGUN FOR VERY HARD X-RAY FREE-ELECTRON LASER

W. H. Tan*, A. Dhar, C. Gunter, J. E. Hernandez Jr., E. Nanni, R. Robles
SLAC National Accelerator Laboratory, Menlo Park, CA, USA

Abstract

X-ray free-electron-laser (FEL) has numerous applications in a wide range of disciplines, such as biology, chemistry and material science. Recently there have been studies on using very hard x-ray FEL to study material properties under extreme conditions. These scientific use cases require FEL photon energies beyond the current state-of-the-art FEL facilities. One pathway of enabling very hard x-ray FEL is to use high gradient radio frequency (rf) driven photogun to deliver bright electron beams. Numerous efforts have been made to push for even higher field gradient while suppressing rf breakdowns. We propose the Compressed Ultrashort Pulse Injector Demonstrator, a 1.6 cell photogun driven by nanosecond high power rf pulses to achieve high gradients with low breakdown rate. This photogun is powered by ultrashort pulses from a rf pulse compressor and a high power klystron. We first show the design of CUPID photogun, followed by its capability of bright beam generation when forming a photoinjector with a superconducting solenoid and downstream linacs. We then use Ming-Xie parameterization to compare FEL performance of CUPID and LCLS nominal injector to demonstrate its improvement in delivering hard x-rays.

INTRODUCTION

The growing interest on very hard x-ray FEL stemmed from the need to understand the mesoscale science, the ability to probe defects of multigranular material and how they behave in extreme conditions [1–6]. Understanding mesoscale science requires x-ray FEL to deliver photon energies at 40 keV and above. One pathway to meet this requirement is use high gradient rf photogun to deliver bright electron beams for FEL [3, 4, 7]. Pushing for higher gradient photogun has been an important topic for bright electron beam generation as the six-dimensional brightness is proportional to the square of the photogun's gradient, where $\mathcal{B}_{6D} = 2I/\varepsilon_n^2\sigma_\gamma \propto E^2$, where I, ε_n, σ_γ and E are the beam current, transverse emittance, normalized rms energy spread and photogun's gradient respectively [8]. We present Compressed Ultrashort Pulse Injector Demonstrator (CUPID), a 1.6 cell photogun that can achieve high gradient with ultrashort high power rf pulses generated by a novel ultra-high power rf pulse compressor, followed the successful demonstration of high gradient short pulse photogun driven by two-beam acceleration method at the Argonne Wakefield Accelerator (AWA) facility [9]. This photogun operates at 11.424 GHz to utilize an available X-band klystron of the same frequency and rf pulse compressor recently commissioned at SLAC [10].

* whtan@slac.stanford.edu

PHOTOGUN DESIGN

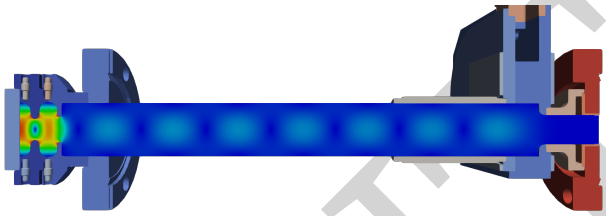

Figure 1: Cut-away view of the relative spacing between the CUPID photogun, the connecting waveguide, and the TM_{10} mode launcher, with superimposed π-mode field map. The relatively long waveguide connecting both components is a design choice to accommodate the physical size of a solenoid designed for bright beam generation. Extended waveguide and solenoid are not shown in this view.

Figure 1 shows the cut-away view of our CUPID photogun, the connecting waveguide and the TM01 mode launcher, with superimposed π-mode field map. The relatively long waveguide connecting both components is a design choice to accommodate the physical size of a solenoid designed to achieve bright electron beams. CUPID photogun achieves high gradient with short rf pulses by having a very short filling time t_{fill}, where it is related to the designed loaded Q-factor, $Q_{\text{load}} = \pi f t_{\text{fill}}$, where f is the operating frequency. Table 1 shows design parameters of CUPID photogun.

Table 1: Design Parameters of CUPID Photogun

Parameter	Value	Unit
Frequency	11.424	GHz
Q_{load}	215	-
S_{11}	–0.59	dB
Field gradient at cathode	500	MV/m
Peak input power	275	MW

BEAM DYNAMICS

Photoinjector Design

In this section we present beam dynamics studies of CUPID photoinjector, it consists of CUPID photogun, enclosed by a superconducting solenoid and connected to downstream S-band linacs. The superconducting solenoid is paired with a bucking solenoid at the back to achieve zero-magnetic field at the cathode to prevent the generation of magnetized beam.

The downstream S-band linacs consist of three accelerating structures, and cryo-cooled to achieve a high gradient field [11]. As shown in Fig. 2, rf pulses generated from a klystron are compressed to high power short pulses, which then sent fo a rf hybrid coupler where one of the output ports is connect to CUPID photogun and the other is connected to a rf load. Another rf load is connected to the last port to prevent reflected pulses from damaging the klystron. A future design is planned to incorporate rf hybrid coupler and TM01 mode launcher to allow efficient use of compressed pulses.

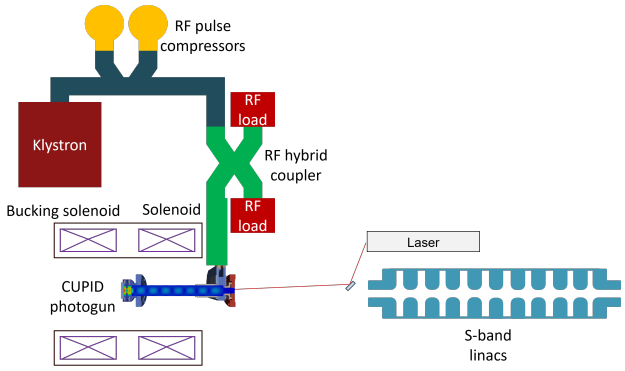

Figure 2: Rf pulses generated from the klystron (red box) is compressed by rf pulse compressors (yellow circles) into high power short rf pulses, which then sent to the rf hybrid coupler. Rf pulses are split into two output ports, where one of them is connected to our CUPID photogun. The other output port is connected to a rf load. Since more than 95 % of rf power will be reflected from CUPID photogun, another rf load is connected to the last port of the hybrid coupler to prevent reflected pulses from damaging the klystron. CUPID photogun is enclosed by a superconducting solenoid and connected to downstream S-band linacs.

Beam Dynamics Results

We performed beam dynamics simulations of CUPID photoinjector using General Particle Tracer (GPT) [12] with 500 000 macroparticles. We were interested in the generation of high brightness beams at 100 pC total charge. The initial beam distribution had a mean transverse energy (MTE) of 400 meV, which corresponds to the thermal emittance of 0.9 µm/mm, given by

$$\frac{\varepsilon_n}{\sigma_x} = \sqrt{\frac{\mathrm{MTE}}{mc^2}}, \tag{1}$$

where σ_x is the laser spot size [13]. The beam was assumed to have a uniform radial and flat top temporal distribution. Table 2 summarized optimized photoinjector's and final beam's parameters. We achieved 63 nm transverse emittance using our CUPID photoinjector. Figure 3 shows the evolution of beam's emittance (red line) and rms beam size (green line) of CUPID photoinjector. The slice emittance of the beam's core is at 40 nm, as shown in Fig. 4.

Table 2: Optimized Parameters for the Injector and Generated Beam Parameters

Parameter	Value	Unit
Laser spot size	70	µm
Laser duration	4.5	ps
Mean transverse energy	400	meV
Beam charge	100	pC
Gun frequency	11.424	GHz
Field on cathode	500	MV/m
Injection phase	70	°
Linacs frequency	2.856	GHz
Linac 1 gradient	100	MV/m
Linac 1 phase (from on-crest)	−3.3	°
Linac 1 distance from the cathode	0.6	m
Linac 2 gradient	100	MV/m
Linac 2 phase (from on-crest)	0	°
Linac 3 gradient	44	MV/m
Linac 3 phase (from on-crest)	0	°
Solenoid field	0.62	T
Solenoid center from the cathode	0.05	m
Final beam energy	135	MeV
Final beam bunch length	342	µm
Final beam rms size	136	µm
Final beam transverse emittance	63	nm
Final beam relative energy spread	0.04	%

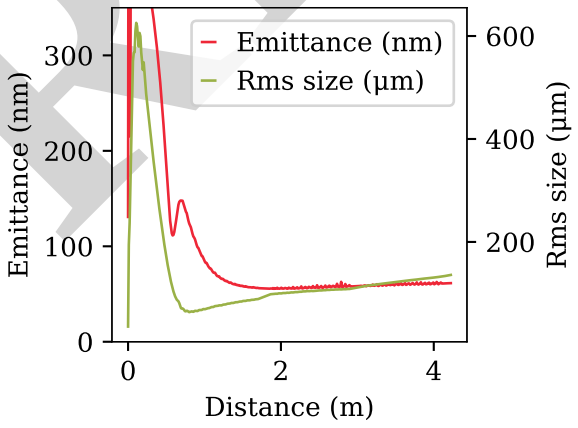

Figure 3: The evolution of beam's emittance (red line) and rms beam size (green line) of CUPID photoinjector using parameters shown in Table 2.

FEL PERFORMANCE ANALYSIS WITH MING-XIE PARAMETERIZATION

Having obtained low emittance beams from CUPID photoinjector, we investigated the performance gain of CUPID photoinjector over the present LCLS injector for FEL. For simplicity, we used the Ming-Xie parameterization analysis to calculate the performance gain [14]. Undulator parameter K_u were adjusted to match the FEL resonance condition,

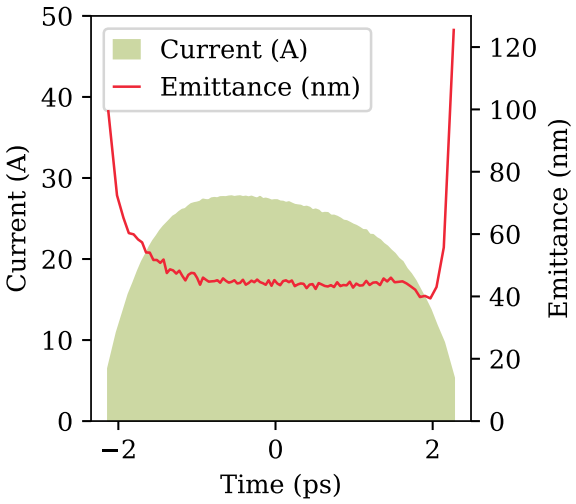

Figure 4: Current profile (green shaded region) and slice emittance (red line) of the beam at the end of CUPID photoinjector. The core emittance (at center) is 40 nm.

using

$$\lambda_{\mathrm{ph}} = \frac{\lambda_u}{2\gamma^2}\left(1 + \frac{{K_u}^2}{2}\right), \tag{2}$$

where λ_{ph} is the wavelength of x-ray photon, λ_u is the undulator period, γ is the beam's Lorentz factor, K_u is the undulator parameter. We assumed that beams from CUPID photoinjector can achieves average current of 1600 A with emittance growth to 100 nm, whereas LCLS beams at 2200 A and 400 nm. Table 3 summarizes parameters that we used for our Ming-Xie analysis. Figure 5 shows the result where CUPID beams maintain more than 0.1 mJ pulse energy up to 60 keV photon energy and outperform LCLS injector.

Table 3: Parameters used for Ming-Xie Parameterization

Parameter	Value	Unit
Undulator period λ_u	26	mm
Beam energy	14.5	GeV
Beta function β_x	5	m
relative energy spread	0.009	%
Current (CUPID)	1600	A
Current (LCLS injector)	2200	A
Emittance (CUPID)	100	nm
Emittance (LCLS injector)	400	nm
Charge duration (CUPID)	45	fs
Charge duration (LCLS injector)	80	fs

CONCLUSION

In summary, we present CUPID, a 1.6 cell high gradient short pulse driven photogun capable of delivering low emittance beams, down to 63 nm. Using Ming-Xie parameterization and assumptions of emittance growth to 100 nm,

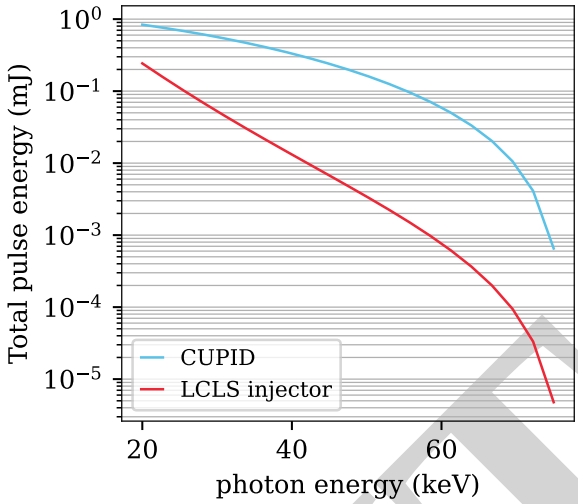

Figure 5: Comparison of hard x-ray FEL performance at different photon energies in terms of total pulse energy using Ming-Xie parameterization. CUPID (blue line) outperforms LCLS nominal (red line). CUPID maintains more than 0.1 mJ pulse energy up to 60 keV photon energy.

we showed that CUPID beams outperform LCLS nominal beams especially as we go to higher photon energies. Detailed studies using dedicated FEL simulation codes will be planned to obtain more accurate performance gain.

ACKNOWLEDGMENTS

This work is supported by the U.S. Department of Energy Contract No. DE-AC02-76SF00515 with SLAC National Accelerator Laboratory. Simulation works used resources of the National Energy Research Scientific Computing (NERSC) Center, U.S. Department of Energy Office of Science User Facility located at Lawrence Berkeley National Laboratory, operated under Contract No. DE-AC02-05CH11231.

REFERENCES

[1] G. Crabtree *et al.*, "From quanta to the continuum: opportunities for mesoscale science", USDOE Office of Science (SC) (United States), Rep., Sep. 2012. doi:10.2172/1183982

[2] J. L. Barber, C. W. Barnes, R. L. Sandberg, and R. L. Sheffield, "Diffractive imaging at large fresnel number: challenge of dynamic mesoscale imaging with hard x rays", *Phys. Rev. B*, vol. 89, no. 18, p. 184105, May 2014. doi:10.1103/PhysRevB.89.184105

[3] RL. Sheffield, CW. Barnes, and JP. Tapia, "Matter-Radiation Interactions in Extremes (MaRIE) project overview", in *Proc. of International Free Electron Laser Conference (FEL'17)*, Santa Fe, NM, USA, pp. 24–28. doi:10.18429/JACoW-FEL2017-MOD06

[4] B. E. Carlsten, P. M. Anisimov, C. W. Barnes, Q. R. Marksteiner, R. R. Robles, and N. Yampolsky, "High-brightness beam technology development for a future dynamic mesoscale materials science capability", *Instruments*, vol. 3, no. 4, 2019. doi:10.3390/instruments3040052

[5] R. G. Kraus, D. Dattelbaum, and M. Knudson, "NNSA light source enhancements: coupling a high energy laser driver to an XFEL", Lawrence Livermore National Laboratory (LLNL), Livermore, CA (United States), Rep., Nov. 2021. doi:10.2172/1835032

[6] A. Benuzzi-Mounaix *et al.*, "Scientific opportunities with very hard xfel radiation", Schenefeld. 2024, Rep. REPORT. XFEL.EU WR-2024-002, 2024. doi:10.22003/XFEL.EU-WR-2024-002

[7] X. Wang, P. Musumeci, E. Lessner, and J. Goldstein, "Report of the basic energy sciences workshop on the future of electron sources, september 8-9, 2016", USDOE Office of Science (SC) (United States), Rep., Sep. 2016. doi:10.2172/1616511

[8] J. B. Rosenzweig *et al.*, "An ultra-compact x-ray free-electron laser", *New J. Phys.*, vol. 22, no. 9, p. 093067, Sep. 2020. doi:10.1088/1367-2630/abb16c

[9] W. H. Tan *et al.*, "Demonstration of sub-GV/m accelerating field in a photoemission electron gun powered by nanosecond *X*-band radio-frequency pulses", *Phys. Rev. Accel. Beams*, vol. 25, no. 8, p. 083402, Aug. 2022. doi:10.1103/PhysRevAccelBeams.25.083402

[10] A. Dhar, M. Othman, and V. Dolgashev, "Development of ultra high power compact x-band pulse compressor", in *Proc. IPAC'25*, Taipei, Taiwan, pp. 1933–1936. doi:10.18429/JACoW-IPAC25-WEPB100

[11] A. Dhar *et al.*, "Distributed coupling linac for efficient acceleration of high charge electron bunches", in *Proc. IPAC'24*, Nashville, TN, USA, pp. 1448–1450. doi:10.18429/JACoW-IPAC2024-TUPR14

[12] Pulsar. Physics, General Particle Tracer (GPT), 2025, https://www.pulsar.nl/gpt

[13] D. H. Dowell and J. F. Schmerge, "Quantum efficiency and thermal emittance of metal photocathodes", *Phys. Rev. ST Accel. Beams*, vol. 12, no. 7, p. 074201, Jul. 2009. doi:10.1103/PhysRevSTAB.12.074201

[14] M. Xie, "Design optimization for an X-ray free electron laser driven by SLAC LINAC", in *Proceedings Particle Accelerator Conference*, Dallas, TX, USA, May 1995, pp. 183–185. doi:10.1109/PAC.1995.504603